Lattice dynamics of HgSe: Neutron scattering measurements and *ab initio* studies

J. Łażewski and K. Parlinski
Institute of Nuclear Physics, Radzikowskiego 152, 31–342 Kraków, Poland

W. Szuszkiewicz
Institute of Physics, Polish Academy of Sciences, Al. Lotników 32/46, 02–668 Warszawa, Poland

B. Hennion
Laboratoire Léon Brillouin, CEA–CNRS, CE Saclay, 91191 Gif-sur-Yvette Cedex, France
(Received 10 July 2002; revised manuscript received 21 January 2003; published 31 March 2003)

The phonon dispersion relations of HgSe, which is a cubic polar semiconductor with a zero energy gap, has been investigated by means of the coherent inelastic neutron scattering. The complete set of phonon branches has been determined along the [001], [110], and [111] high-symmetry directions. Using the *ab initio* local-density approximation with ultrasoft pseudopotentials, we have calculated the Hellmann–Feynman forces for $2\times2\times2$ supercell. Applying the direct method, the phonon dispersion relations and the phonon density of states have been derived. They are in good agreement with the results of the neutron-scattering data. The $1\times1\times10$ elongated supercell has been used to find the LO/TO splitting of the optical phonon branches for two different concentrations of free carriers. Higher free-carriers density diminish the LO/TO splitting.

DOI: 10.1103/PhysRevB.67.094305 PACS number(s): 63.20.−e, 25.40.Fq, 07.05.Tp

I. INTRODUCTION

Mercury selenide, HgSe crystallizes in the cubic zinc-blende structure ($F\bar{4}3m$). It is a well-known II-VI semiconducting compound with an inverted band structure. Strictly speaking, due to the lack of energy gap between the valence and the conduction bands HgSe is a zero-gap semiconductor.[1,2] At the same time, because of the high nonparabolicity of the conduction band, which results from the small distance between the top of the light-hole and the heavy-hole valence bands, this compound belongs to the group of narrow-gap semiconductors.

Even ''pure'' HgSe is an n-type semiconductor with a free-carrier concentration typically close to 2×10^{18} cm^{-3}. Such a high concentration is thought to be related to numerous defects created in crystal during the growth process. In this material the Fermi energy is always lying well within the conduction band. Thus, HgSe is often called ''semimetal'' in spite of the fact that for a real semimetal the bottom of a conduction band is slightly below the top of a valence band, and therefore one expects a significant concentration of free carriers—electrons or holes.

HgSe has attracted a lot of attention in the last few years. Indeed important progress in molecular beam epitaxy growth of mercury compounds make it possible to produce not only thin layers,[3–5] but also HgSe-based quantum structures like quantum wells,[6] quantum wires[7] and, recently, even quantum dots[8] which could result in possible applications in near future. On the other hand, results of precise photoemission studies performed for pure HgSe crystals[9,10] seemed to be in contradiction with the well established zero-gap character of this compound. Of course such a suggestion stimulates an increasing interest in various properties of HgSe.

The semimetallic nature of HgSe has been checked once more and analyzed by means of conductivity, optical and magnetooptical measurements[11] as well as by *ab initio* quasiparticle band-structure calculations[12] and optical response calculations with scalar relativistic effects.[13] Very low photoemission intensity observed just above the valence-band maximum, which has been used as an argument in favor of narrow positive gap,[9] was attributed to a very light effective mass and low electronic density of states (eDOS) of the lowest conduction band.[13]

HgSe is a semiconducting compound which exhibits a lot of peculiar properties. Due to the finite free-carrier concentration, a dielectric function anomaly, as a direct consequence of the lack of the energy gap, is observed in numerous transport[14] and optical[15] measurements, although these effects are less pronounced for HgSe than for example for HgTe. The difference of the atomic masses of Hg and Se has an important influence on the lattice dynamics. The lack of the energy gap in eDOS allows for a two-phonon resonant effect.[16] This effect was assumed to be responsible for the observed anomalies in the far-infrared reflectivity[17] but recent neutron-scattering and Raman-scattering data suggest rather that an additive two-phonon process could explain these anomalies.[18] The temperature dependence of the distance between the top of the heavy-hole and the light-hole valence bands, which plays a role of a narrow ''band gap,'' could also be connected with the behavior of a phonon acoustic mode.[19] Also some low-temperature behavior in the heat capacity are strongly related to the acoustic phonon dispersion relations.[20] All effects listed above can be explained by the presence of low-energy, weak-dispersive transverse acoustic modes observed in this compound.

Another interesting properties of HgSe result from its high ionicity $F=0.68$.[21] As it is known $F_c=0.785$ is the critical ionicity that separates the fourfold and sixfold coordinated crystal structures.[22] The ionicity values for all mercury chalcogenides are close to F_c. Strictly speaking, HgSe with the ionicity below this value crystallizes still in the zinc-blende structure, while the stable structure of slightly

more ionic mercury sulphide HgS has the cinnabar hexagonal structure. In particular, relatively large effective charges in HgSe result in the significant LO/TO splitting at the Γ point of the Brillouin zone.

The aim of this work is to report new coherent inelastic neutron-scattering measurements, which provide the complete experimental phonon dispersion curves of HgSe and to derive these phonon dispersion relations and the one-phonon density of states (DOS) from the *ab initio* calculations. Moreover, by changing in the *ab initio* study the free-carrier concentration in the conduction band we found a correlation between this concentration and the magnitude of LO/TO splitting.

The frequencies of the Raman and infrared reflectivity modes at the Γ point of the Brillouin zone as well as some experimental data resulting from the inelastic neutron scattering for acoustic and optical modes have already been described with phenomenological models.[18,23–27] However, to our best knowledge, there are no *ab initio* calculations of the lattice dynamics for semimetallic crystals with such a peculiar band structure. So, one may also consider the comparison of experimental and calculated data as a test of the applicability of the used methods to this type of compounds.

II. EXPERIMENTAL METHODS AND RESULTS

High quality HgSe single crystals were grown from the melt by the vertical Bridgman method in the Institute of Physics of the Polish Academy of Sciences in Warsaw. For the chemical synthesis pure elements (Hg 4N and Se 5N) were used. The crystallization took place in one inch diameter quartz crucibles. Crystal quality was checked by x-ray diffraction and energy dispersive x-ray fluorescence methods, and no precipitates and chemical impurities were detected.

Inelastic neutron-scattering measurements on mercury compounds are hampered by the high neutron absorption of mercury since the absorption cross section is 372 barns. Nevertheless, the high value of the mercury neutron-scattering-length (1.266×10^{-12} cm) allows to get reasonable experimental conditions when using thin sample plates, as demonstrated in earlier measurements for HgTe[24,28,29] and HgSe.[24,29] Two kinds of plates, cut perpendicularly to [001] and [110] directions, were obtained for the HgSe crystals, and used as grown without thermal annealing. The samples of 1 mm thickness had a surface of about 2.5 cm^2. A free-electron concentration equal to $(2.2\pm0.2)\times10^{18}$ cm^{-3} has been estimated from the low-temperature plasma-edge position, measured for one of these plates.[30]

The coherent inelastic neutron-scattering measurements have been performed at the Laboratoire Léon Brillouin in Saclay on the 1 T triple-axis spectrometer, installed on a thermal beam of the Orphee reactor. Both monochromator and analyzer were pyrolytic graphite in (002) reflection. Vertical focusing of the monochromator and combined horizontal and vertical focusing of the analyzer were used to increase scattered intensities. No Soller slit collimators were used, but the natural collimations of about $30'-40'-50'-50'$ yielded an energy resolution of 0.25 THz at zero energy transfer, with $k_f=2.662$ $Å^{-1}$. Here, k_f is the value of the final neutron wave vector, which was kept fixed throughout the measurements. This value allowed us to use a graphite filter, and hence to protect the scattered beam from higher-order contaminations.

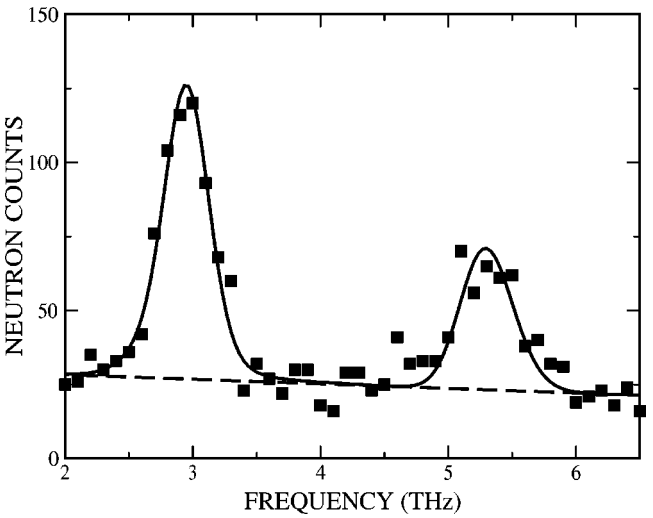

FIG. 1. Neutron counts (squares) of the coherent inelastic neutron scattering from HgSe single crystal at the wave-vector transfer $Q=(2\pi/a_0)(5,0,0)$, corresponding to the X point. The solid line is a profile resulting from a fit of calculated intensity accounting for the experimental resolution function and including two undamped phonon modes (LA and LO, respectively) and a background (dashed line). The measurements were performed at $T=(11.85\pm0.1)$ K.

The inelastic neutron-scattering measurements were carried out along the high-symmetry directions [001], [110], and [111], mainly with the constant Q scans. In order to reduce the phonon damping most of the measurements were performed at low temperatures. The HgSe samples were mounted on the cold finger of a closed cycle refrigerator. For all these measurements the sample was kept in a container with helium exchange gas. Sample temperature was stabilized with an accuracy better than 0.2 K. The measurements were performed between 11 K to 14 K. Some room temperature data were also collected for comparison. The highest observed temperature shift of the phonon frequencies does not exceed 0.15 THz.

Typical experimental data taken at the wave-vector $Q=(2\pi/a_0)(5,0,0)$, which correspond to the X point of the Brillouin zone, are shown in Fig. 1. All the data have been fitted to a calculated profile resulting from the experimental resolution function with a neutron-scattering cross section for undamped phonons plus a background. This modeling accounts for experimental effects related to the dispersion of the modes. The accuracy of the deduced mode position is thus determined by the Gaussian counting statistics. The typical uncertainties are estimated to about 0.03 THz for the less intense optical modes and to about 0.01 THz for the acoustic modes. A systematic shift due to the accuracy of the spectrometer alignment would be less than 0.02 THz. In the most unfavorable case the final accuracy was better than 0.1 THz.

III. *AB INITIO* STUDY: SETUP AND RESULTS

A. Band structure

We have started our *ab initio* study from the calculation of the band structure and eDOS. The used ultrasoft pseudopotentials for Hg and Se atoms represent $5d^{10}6s^2$ and $4s^24p^4$ electron configurations, respectively. For Hg we took into consideration the *d* electrons because of their crucial role in HgSe band structure.[31] This part of the calculations has been carried out with the primitive unit cell containing two atoms. Using the self-consistent charge-density distribution obtained for the optimized structure with $8\times8\times8$ wave-vector grid, the electronic energy levels along the high-symmetry directions in the Brillouin zone have been calculated. We have obtained an inverted gap of about -1 eV, which overestimates the experiment value which is -0.27 eV.[32] Our value is, however, in good agreement with previous *ab initio* calculations.[12,13] De Boeij, Kootstra, and Snijders[13] show that spin-orbit coupling raises Γ_8 bands by about 0.1 eV, increasing the inverted local-density approximation (LDA) gap to -1.1 eV. Within the GW approximation Rohlfing and Louie[12] found that quasiparticle corrections mainly affect the *s*-like states (Γ_6 among others) moving them upwards by about 0.8 eV and reducing the gap. We have also obtained the correct shapes of the Hg 5*d* and Se 4*s* bands at 6 eV and at about -13 eV, respectively. Using the same procedure described above with fairly dense grid of $16\times16\times16$ *k* points, we have calculated eDOS. It agrees very well with the ultraviolet photoemission spectroscopy data.[33]

The above results indicate that the electronic structure of the HgSe crystal is well reproduced. Hence, one can expect that within the same approach the Born effective charges and LO/TO splitting calculations will lead to reasonable results.

B. Phonons

The calculations of the phonon dispersion relations were performed with the direct method.[34–37] The direct method uses the Hellmann-Feynman (HF) forces calculated for optimized supercell with one atom displaced from equilibrium position, derives the force constants using the symmetry elements of the space group of the crystal, and calculates phonon frequencies by diagonalizing the dynamical matrix.

In this work the crystal structure optimization and calculation of HF forces have been performed within the density-functional theory using the pseudopotential method[38] with the LDA,[39] as implemented in VASP software.[40,41] A plane-wave basis set with 200 eV energy cutoff has been applied. All calculations have been done for $2\times2\times2$ and $1\times1\times10$ supercells with 64 and 80 atoms, respectively. The $2\times2\times2$ supercell has been used to find phonon dispersion curves in all directions and the one-phonon DOS, while the elongated supercell allowed us to extract the LO/TO splitting.[42] The integration over the Brillouin zone has been performed with the weighted summation over 4 irreducible wave vectors generated by the Monkhorst-Pack scheme,[43] which corresponds to $2\times2\times2$ *k* point mesh. Because all atoms in zinc-blende structure are in high-symmetry sites the only measure of accuracy of the energy minimum is the external stress. The minimization process has been carried on until external stress decreased below 1 MPa.

The optimized lattice parameter *a*, which follows from the $2\times2\times2$ supercell amounts 6.079 Å, which is comparable with 6.091 Å obtained from the all-electron total-energy calculations using the self-consistent general-potential linearized augmented-plane-waves method.[44] Our lattice parameter is also in a very good agreement with the experimental one 6.085 Å taken at 200 K (see, e.g., review paper Ref. 45). In the case of the zinc-blende structure two independent displacements (one for Hg and one for Se atom) are necessary to obtain a complete set of HF forces. We used displacements of 0.5% of the supercell lattice vector. To minimize systematic errors and eliminate odd order anharmonic effects, sets of positive and negative displacements have been calculated. The cumulant force constants[37] have been found from HF forces by the singular value decomposition method.[46,47] All nonzero force constant elements obtained for $2\times2\times2$ supercell have been listed in Table I. Rigid-ion model parameters taken from Ref. 25 have been added in parenthesis. Our force constants are very similar to those of rigid-ion model. Specially the first neighbor force constants are close to each other. The largest discrepancy occurs on the next-nearest neighbors of Hg atom at off-diagonal component *xy*. The values of the derived force constant elements generally diminish with the distance between related atoms. In the case of $2\times2\times2$ supercell the largest force constants drop down by two orders of magnitude at the distance from the central atom of the supercell to the atom at the supercell surface. The force constants are introduced in the dynamical matrix, which is diagonalized in order to obtain phonon frequencies. Independently of the range of interaction the $2\times2\times2$ supercell provides exact phonon frequencies at Γ, X, L, and W high-symmetry points of the Brillouin zone. These wave vectors are commensurate with the $2\times2\times2$ supercell size.[34,48]

In Fig. 2 we compare our calculated phonon dispersion relations with the present inelastic neutron-scattering measurements along the high-symmetry lines as well as the infrared reflectivity and the Raman-scattering data[18,21,49] at the Γ point. Calculated from $2\times2\times2$ supercell acoustic phonon frequencies along Γ-K-X line overestimate experimental data by about 30%. We believe that it originates from still too small supercell size. Therefore we built up $3\times3\times1$ supercell which gives two additional ''exact'' frequencies on line Γ-K-X at the wave-vectors commensurate with supercell size, $\mathrm{k}=(2\pi/a_0)(\frac{1}{6},\frac{1}{6},0)$ and $\mathrm{k}=(2\pi/a_0)(\frac{1}{3},\frac{1}{3},0)$. The calculated ''exact'' phonon frequencies obtained from $3\times3\times1$ supercell are marked on Fig. 2 with open squares. Next, we slightly modified the force constants matrices of $2\times2\times2$ supercell to fit those four ''exact'' points. Now, a good overall agreement with experimental data is well seen.

The total and partial one-phonon density of states for HgSe are shown in Fig. 3. The high-frequency part originates mainly from the lower-mass atoms Se ($M_{Se}=79$ amu). This band is separated by a wide gap in one-phonon density of states from the low-frequency part which results primarily from the vibrations of the higher-mass atoms Hg ($M_{Hg}=201$ amu). Such behavior differs a lot from the properties

TABLE I. Force constant matrices calculated from $2\times2\times2$ supercell. First atom positions are Hg (0.00, 0.00, 0.00) and Se (0.25, 0.25, 0.25). Numbers in parenthesis are force constants parameters of the rigid-ion model (Ref. 25).

Interacting atoms	Second atom position	Distance in Å	Independent force constants in amu THz^2		
Hg—Hg	(0.00, 0.00, 0.00)	0.00	xx	46010	(30005)
Se—Se	(0.25, 0.25, 0.25)	0.00	xx	70507	(68620)
Hg—Se	(0.25, 0.25, 0.25)	2.63	xx	−11187	(−11024)
			xy	−11855	(−9335)
Hg—Hg	(0.00, 0.50, 0.50)	4.30	xx	3100	(7950)
			yy	−1958	(−1050)
			xy	−1858	(−40000)
			yz	−2178	(−2400)
Se—Se	(0.25, 0.75, 0.75)	4.30	xx	−1063	(−4700)
			yy	−2843	(−2740)
			xy	−421	(−3100)
			yz	−3041	(−2830)
Se—Hg	(0.00, 0.00, 1.00)	5.04	xx	−315	
			zz	779	
			xy	72	
			xz	−395	
			yx	5	
Hg—Hg	(0.00, 0.00, 1.00)	6.08	xx	45	
			zz	−484	
Se—Se	(0.25, 0.25, 1.25)	6.08	xx	111	
			zz	−183	
Hg—Se	(0.25, 0.75, 0.75)	6.62	xx	−299	
			yy	799	
			xy	−673	
			xz	−557	
			yx	−96	
Hg—Hg	(0.50, 0.50, 1.00)	7.45	xx	−94	
			zz	−322	
			xy	88	
			xz	−147	
Se—Se	(0.75, 0.75, 1.25)	7.45	xx	−51	
			zz	−222	
			xy	−34	
			xz	−27	
Se—Hg	(1.00, 1.00, 1.00)	7.90	xx	278	
			xy	−54	
Hg—Hg	(0.00, 1.00, 1.00)	8.60	xx	446	
			yy	−188	
Se—Se	(0.25, 1.25, 1.25)	8.60	xx	55	
			yy	−398	
Hg—Hg	(1.00, 1.00, 1.00)	10.53	xx	−40	
Se—Se	(1.25, 1.25, 1.25)	10.53	xx	−23	

of typical semiconductor like, e.g., GaAs, but it simply results from the difference of the atomic masses of both constituents.

C. LO/TO splitting

At the Γ point of the Brillouin zone the optical modes correspond to relative motion of the Hg and Se sublattices. In polar crystals such as HgSe, the optical modes induce a dipole moment. The dipole moment of the TO mode is perpendicular to the wave-vector **k**. The LO mode induces a dipole moment parallel to the wave-vector **k**, and this mode generates a macroscopic electric field. Being perpendicular to **k**, the dipole moment of TO mode is not influenced by the macroscopic electric field, in contrary to the LO mode which

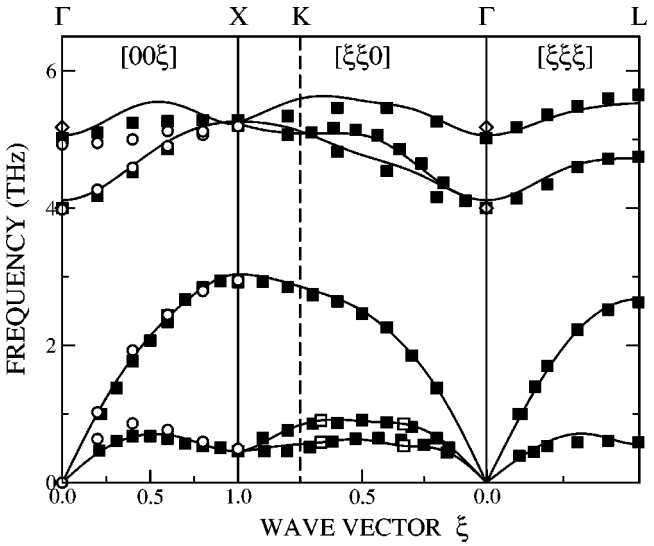

FIG. 2. Comparison of the calculated phonon dispersion relations of the zinc-blende HgSe with experimental data (filled squares). Diamonds are frequencies obtained from Raman-scattering and infrared reflectivity measurements (Refs. 21,18,49). Lines and open circles indicates results obtained from $2\times2\times2$ and $1\times1\times10$ supercells, respectively.

frequency is changed by the coupling to this field. The LO/TO splitting of phonon frequencies arises in the Γ point of Brillouin zone. The Ewald summation used in the *ab initio* calculations precludes a generation of a macroscopic electric field and hence the calculated phonon frequency at the Γ point corresponds to the TO modes only. In Refs. 50 and 51 we have considered cubic MgO and BN crystals and we have shown that the elongated supercell may be used to find the LO/TO splitting by extrapolation of the longitudinal optical phonon branch to $\mathbf{k}=0$ wave vector. Following this approach we use for HgSe the $1\times1\times10$ elongated supercell. In this case for the summation over the Brillouin zone of the electronic states, we use the tetrahedron method with 39 tetrahedra based on 9 *k*-points generated from $5\times5\times1$ mesh by the Monkhorst-Pack scheme. The phonon dispersion curves were recalculated using HF forces generated by the *x* and *z* displacements, one at the time for Hg and Se atoms. From such an elongated supercell one obtains reliable phonon frequencies along the Γ-*X* line at the wave-vectors k_n $=(2\pi/a_0)(0,0,n/10)$, except for LO mode at $\mathbf{k}=0$. Here *n* is an integer number. The phonon frequencies between these special k_n points have no physical meaning. The extrapolation of the LO phonon branch to $\mathbf{k}=0$ gives the frequency equal to 4.9 THz, which should be compared with the value 5.02 THz, obtained from inelastic neutron scattering.

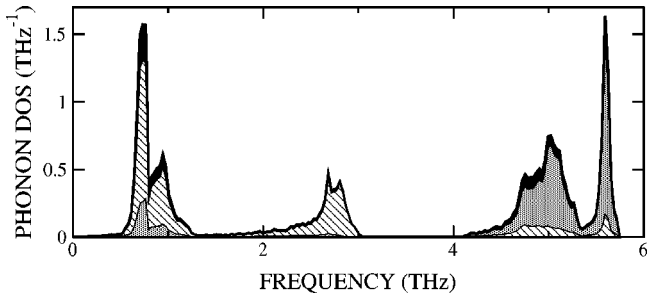

FIG. 3. Calculated one-phonon density of states (DOS) for HgSe. Black, hashed, and dotted area indicate total, partial for Hg and partial for Se DOS, respectively. The distributions are normalized to 1, $\frac{1}{2}$, and $\frac{1}{2}$, respectively.

The LO phonon frequency allows to calculate the ratio of the Born effective charge tensor $\mathbf{Z}^*$ to the square root of the electronic part of the dielectric constant ε_∞, i.e., $\mathbf{Z}^*/\sqrt{\varepsilon_\infty}$. For that one adds to the dynamical matrix the nonanalytical term proposed by Pick, Cohen, and Martin.[52] This term depends on $\mathbf{Z}^*/\sqrt{\varepsilon_\infty}$ tensor and describes the LO mode at $\mathbf{k}=0$. The octahedral site point group of Hg and Se atoms guarantees that the effective charge tensor is diagonal and the diagonal elements are equal. The values derived from LO phonon frequency of 4.9 THz reads $Z^*_{Hg}/\sqrt{\varepsilon_\infty}=-Z^*_{Se}/\sqrt{\varepsilon_\infty}=0.79$.

On the other hand from the theory of the crystal polarization proposed by Resta[53] one can calculate the Born effective charges $\mathbf{Z}^*$ using the Berry phase method.[54,55] In zinc-blende structure there are only two independent displacements needed, one for each atom. We chose the displacement amplitude of 0.05 Å. We obtained $Z^*_{Hg}=-Z^*_{Se}=3.44$, which leads to $\varepsilon_\infty=19$. This value can be compared with $Z^*_{Hg}=3.92$ or 3.95 reported in Refs. 56 and 21, respectively. Present value of ε_∞ is also in a reasonable agreement with the results of the analysis of the dynamic dielectric function for HgSe, presented in Refs. 15 and 17.

In Fig. 2 we show the phonon dispersion curves calculated from $2\times2\times2$ supercell with the nonanalytical term included. The longitudinal optical phonon branch is interpolated between LO mode at $\mathbf{k}=0$ found from the $1\times1\times10$ elongated supercell and the zone boundary modes which are calculated exactly from the $2\times2\times2$ supercell. We show points obtained from elongated supercell along the Γ-*X* direction. Let us remind that these phonon frequencies at k_n wave vectors, for $1\leqslant n\leqslant5$, are calculated without the nonanalytical term. The slight differences between transverse (TA and TO) phonon frequencies calculated with two supercells are mainly due to numerical errors and slightly different conditions used to evaluate the *ab initio* HF forces.

IV. DISCUSSION AND CONCLUSIONS

We can state that the *ab initio* phonon dispersion calculations based on the direct method agree very well with the inelastic neutron-scattering measurements for HgSe. The calculations well reproduce the flat behavior of the transverse acoustic modes. Moreover, the LO/TO splitting, being always a difficult part of the direct method calculations, is correctly derived from the elongated supercell.

In spite of its semimetallic character and inverted band structure with a zero energy gap HgSe is a polar crystal in which the LO/TO splitting is observed experimentally. It means that its electronic part of the dielectric constant has a finite value. On the other hand our sample is not an insulator, but contains about 2.2×10^{18} free carriers per cm^3. If one would be able to convert this crystal into a metal, by increas-

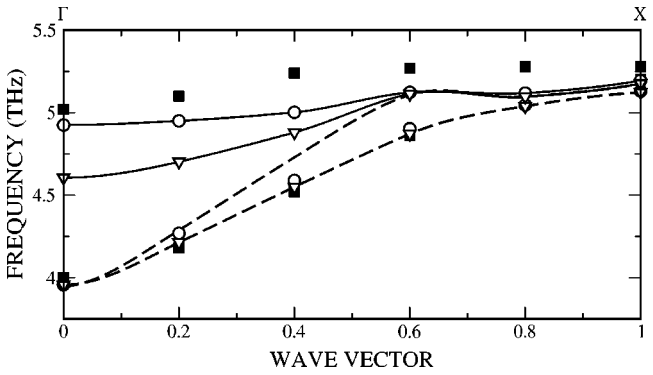

FIG. 4. Calculated optical phonons dispersion relations along Γ-X direction. Open circles and triangles correspond to the state with 1.7×10^{19} cm^{-3} and 1×10^{20} cm^{-3} free-carrier concentrations, respectively. Lines are guides to the eyes. Dashed lines correspond to the metallic system for which no splitting is expected.

ing the electron density in the vicinity of the Fermi energy, then one should obtain an infinite electronic part of the dielectric constant, and the LO/TO splitting will disappear. A small change in the occupancy of the electronic states in the conduction band in the vicinity of the Γ point would increase the Fermi energy, which would enter the region of finite density of states. Then the electronic part of the dielectric constant would tend to infinity, and the LO/TO splitting will drop down to zero. Thus, by changing the free-carrier concentration in the conduction band, one should be able to modify (decrease or even remove) the LO/TO splitting.

The band structure of HgSe consists of a pair of Γ_8 bands at the Fermi level. The elongated supercell calculations referred in Sec. III C were carried out under the assumption that in the ground state this pair of the doubly degenerate Γ_8 bands is occupied by 2 electrons, one on each Γ_8 band. Taking into account finite summations over discrete **k** points in the Brillouin zone one can estimate the concentration of the free carriers in such a calculation to be of about 1.7×10^{19} per cm^3.

In other calculation we have excited one electron to the empty Γ_8 band with higher energy and with wave vector slightly away from $\mathbf{k}=0$, and repeated the phonon calculations. It means that one electron has been excited at additional four, symmetry related, wave vector sout of the set of 25 **k** points of the Brillouin zone. As a consequence of this excitation the concentration of the free-carriers increased up to 1×10^{20} cm^{-3}, but the LO/TO splitting decreased, as seen in Fig. 4. It proves that an increase of the electron carrier density at the Fermi-level introduces a significant change of the frequency of the longitudinal optical phonon. On the same Fig. 4 using dashed line the layout of unsplitted modes has been depicted. The unsplitted mode corresponds to a metallic state with infinite value of dielectric constant ε_∞. Still an open question remains whether a decrease of LO/TO splitting with an increase of concentration of free carriers may be observed experimentally. The free-carrier concentration for a typical metal is of order of 10^{22} cm^{-3} which is a four orders of magnitude higher than the free-electron concentration in our sample. It is known that by proper HgSe annealing or doping, one could obtain crystals with a free-electron concentration ranging from 3.6×10^{16} cm^{-3} (at $T=4.2$ K) or 4×10^{17} cm^{-3} (at $T=295$ K)[56] to 3×10^{19} cm^{-3}.[14] Hence, even the highest free-electron concentration does not allow to expect a significant changes of the LO/TO splitting. Nevertheless, according to the theoretical estimation presented in Fig. 4, the LO phonon frequency at the Brillouin zone center decreases by about 0.3 THz, when increasing the free-carrier concentration form 1.7×10^{19} to 1×10^{20} cm^{-3}. If so, one should expect a difference of the order of 0.1 THz when comparing the results of present model and possible experimental data for HgSe sample with the highest available concentration. We believe it could be detected by optical measurements.

It should be pointed out that a large LO/TO splitting is not characteristic of highly ionic semiconductors, although it is known for crystals like CuCl.[57] However, the influence of the free-carrier concentration on the optical phonon branches can be observed for narrow-gap semiconductors only. High doping should be used to shift the position of the Fermi level not only in order to create the degenerated material but also to change significantly its ''energy gap'' for the interband optical transitions. The compound should have a high value of the dielectric constant to ensure that not only the intraband part of the dielectric function but also the interband contribution to this function is significantly modified by the high doping.

Presently we know two groups of materials which are able to satisfy the above mentioned conditions and for which one can expect such characteristics. The first group consists of IV-VI narrow-gap semiconductors (lead chalcogenides). Their dielectric constants have extremely high values. Because of a large number of defects they also have a high free-carrier concentration. The lattice dynamics determined[58,59] for PbS and PbTe deviate indeed from the normal ionic behavior because of the screening effects due to free-carriers present in these crystals. The second group of compounds is that of mercury chalcogenides. In this case the LO-phonon screening has been observed by neutron scattering for *p*-type HgTe.[24,29] However, up to now the quantitative description of the screening effect has been limited to the analysis of the appropriate contributions to the dynamic dielectric function in the case[60] of PbS and HgTe.[24,29] Our calculations show that this effect can be directly obtained for a semiconductor by *ab initio* calculations.

In summary we can conclude that the *ab initio* calculations presented in this paper are able to describe the lattice dynamics of a zero-gap semiconductor like HgSe. The results of these calculations reproduce well principal peculiarities of HgSe phonon dispersion relations in spite of a semimetallic character of this compound.

ACKNOWLEDGMENTS

The authors would like to express their gratitude to B. Witowska for growing the HgSe monocrystals, to E. Dynowska and J. Górecka for the x-ray diffraction measurements, to P. T. Jochym and A. Fleszar for fruitful discussions, and to M. Marsman for implementation of the Berry phase

procedure. This work was partially supported by the State Committee of Scientific Research (KBN), Grant No. 5P03B 069 20. The computational grant from ACC Cyfronet Cracow No. KBN/SGI2800/IFJ/102/2001 is kindly acknowledged. This work was also supported in part within European Community program Grant No. ICA1-CT-2000-70018 (Center of Excellence CELDIS) and within European Commission through the Access to Research Infrastructures Action of the Improving Human Potential Program (Contract No. HPRI-CT-1999-00023).

[1] A. Mycielski, J. Kossut, M. Dobrowolska, and W. Dobrowolski, J. Phys. C **15**, 3293 (1982).
[2] T. Dietl, W. Dobrowolski, J. Kossut, B.J. Kowalski, W. Szuszkiewicz, Z. Wilamowski, and A.M. Witowski, Phys. Rev. Lett. **81**, 1535 (1998).
[3] S. Einfeldt, H. Heinke, M. Behringer, C.R. Becker, E. Kurtz, D. Hommel, and G. Landwehr, J. Cryst. Growth **138**, 471 (1994).
[4] Th. Widmer, D. Schikora, C. Prott, B. Schottker, K. Lischka, S. Luther, and M. von Ortenberg, Semicond. Sci. Technol. **10**, 1264 (1995).
[5] L. Parthier, H. Wissmann, S. Luther, G. Machel, M. Schmidbauer, R. Koehler, and M. von Ortenberg, J. Cryst. Growth **175/176**, 642 (1997).
[6] H. Wissmann, L. Parthier, G. Machel, S. Luther, M. Schmidbauer, R. Kohler, and M. von Ortenberg, *Proceedings of the Eighth International Conference on Narrow Gap Semiconductors* (World Scientific, Singapore, 1998), p. 97.
[7] T. Tran Anh, H. Wissmann, S. Rogaschewski, and M. von Ortenberg, J. Cryst. Growth **214-215**, 40 (2000).
[8] T. Tran Anh, S. Rogaschewski, S. Hansel, A. Kirste, H.-U. Mueller, and M. von Ortenberg, *Proceedings of 26th International Conference Phys. Semicond., Edinburgh*, 2002 (unpublished).
[9] K.-U. Gawlik, L. Kipp, M. Skibowski, N. Orlowski, and R. Manzke, Phys. Rev. Lett. **78**, 3165 (1997).
[10] K.-U. Gawlik, L. Kipp, M. Skibowski, N. Orlowski, and R. Manzke, Phys. Rev. Lett. **81**, 1536 (1998).
[11] M. von Truchsess, A. Pfeuffer-Jeschke, C.R. Becker, G. Landwehr, E. Barke, Phys. Rev. B **61**, 1666 (2000).
[12] M. Rohlfing and S.G. Louie, Phys. Rev. B **57**, R9392 (1998).
[13] P.L. de Boeij, F. Kootstra, and J.G. Snijders, Int. J. Quantum Chem. **85**, 449 (2001).
[14] T. Dietl and W. Szymańska, J. Phys. Chem. Solids **39**, 1041 (1978).
[15] W. Szuszkiewicz, A.M. Witowski, and M. Grynberg, Phys. Status Solidi B **87**, 637 (1978).
[16] A.M. Witowski and M. Grynberg, Solid State Commun. **30**, 41 (1979).
[17] A.M. Witowski and M. Grynberg, Phys. Status Solidi B **100**, 1649 (1980).
[18] W. Szuszkiewicz, E. Dynowska, J. Gorecka, B. Witkowska, M. Jouanne, J.F. Morhange, C. Julien, and B. Hennion, Phys. Status Solidi B **215**, 93 (1999).
[19] R. Dornhaus and G. Nimtz, in *Springer Tracts in Modern Physics*, edited by G. Höhler and E. A. Niekisch (Springer-Verlag, Berlin, 1983), Vol. 98, p. 119.
[20] J.G. Collins, G.K. White, J.A. Birch, and T.F. Smith, J. Phys. C **13**, 1649 (1980).
[21] K. Kumazaki, Phys. Status Solidi B **151**, 353 (1989).
[22] J.C. Phillips Rev. Mod. Phys. **42**, 317 (1970).
[23] A. Manabe and A. Mitsuishi, Solid State Commun. **16**, 743 (1975).
[24] H. Kepa, T. Giebultowicz, B. Buras, B. Lebech, and K. Clausen, Phys. Scr. **25**, 807 (1982).
[25] D.N. Talwar and M. Vandevyver, J. Appl. Phys. **56**, 2541 (1984).
[26] W. Szuszkiewicz, K. Dybko, E. Dynowska, J. Gorecka, B. Witkowska, B. Hennion, M. Jouanne, and C. Julien, Acta Phys. Pol. A **92**, 1029 (1997).
[27] W. Szuszkiewicz, K. Dybko, B. Hennion, M. Jouanne, C. Julien, E. Dynowska, J. Gorecka, and B. Witkowska, J. Cryst. Growth **184**, 1204 (1998).
[28] H. Kepa, W. Gebicki, T. Giebultowicz, B. Buras, and K. Clausen, Solid State Commun. **34**, 211 (1980).
[29] H. Kepa, T. Giebultowicz, B. Buras, B. Lebech, and K. Clausen, in *Lecture Notes in Physics*, edited by E. Gornik, H. Heinrich, L. Palmetshofer (Springer, Berlin, 1982), Vol. 152, p. 276.
[30] W. Szuszkiewicz, M. Arciszewska, B. Witkowska, C. Julien, and M. Balkanski, J. Magn. Magn. Mater. **140-144**, 2037 (1995).
[31] S.-H. Wei and A. Zunger, Phys. Rev. B **37**, 8958 (1988).
[32] M. Dobrowolska, W. Dobrowolski, and A. Mycielski Solid State Commun. **34**, 441 (1980).
[33] D. Eich, D. Hübner, R. Fink, E. Umbach, K. Ortner, C.R. Becker, G. Landwehr, and A. Fleszar, Phys. Rev. B **61**, 12666 (2000).
[34] W. Frank, C. Elsässer, and M. Fähnle, Phys. Rev. Lett. **74**, 1791 (1995).
[35] G. Kresse, J. Furthmüller, and J. Hafner, Europhys. Lett. **32**, 729 (1995).
[36] K. Parlinski, Z.Q. Li, and Y. Kawazoe, Phys. Rev. Lett. **78**, 4063 (1997).
[37] K. Parlinski, in *Neutrons and Numerical Methods-N_2M*, edited by M. R. Jonson, G. J. Kearley and H. G. Büttner, AIP Conf. Proc. No. 479, (AIP, Woodbury, NY, 1999), p. 121.
[38] M.C. Payne, M.P. Teter, D.C. Allan, T.A. Arias, and J.D. Joannopoulos, Rev. Mod. Phys. **64**, 1045 (1992).
[39] J.P. Perdew, J.A. Chevary, S.H. Vosko, K.A. Jackson, M.R. Pederson, D.J. Singh, and C. Fiolhais, Phys. Rev. B **46**, 6671 (1992).
[40] G. Kresse and J. Hafner, Phys. Rev. B **47**, 558 (1993); **49**, 14251 (1994).
[41] G. Kresse and J. Furthmüller, Software VASP, (IMP-UW, Vienna, 1999); G. Kresse and J. Furthmüller, Phys. Rev. B **54**, 11 169 (1996); Comput. Mater. Sci. **6**, 15 (1996).
[42] R. Resta and K. Kunc, Phys. Rev. B **34**, 7146 (1986).
[43] H.J. Monkhorst and J.D. Pack, Phys. Rev. B **13**, 5188 (1976).
[44] Z.W. Lu, D. Singh, and H. Krakauer, Phys. Rev. B **39**, 10 154 (1989).
[45] R.C. Sharma, Y.A. Chang, and C. Guminski, J. Phase Equilib. **13**, 663 (1992).
[46] W. H. Press, S. A. Teukolsky, W. T. Vetterling, and B. P. Flannery,

Numerical Recepies (Cambridge University Press, Cambridge, 1992), p. 670.
[47] K. Parlinski, computer code PHONON (Cracow, Poland, 2001).
[48] B. Meyer, V. Schott, and M. Fähnle, Phys. Rev. B **58**, R14673 (1998).
[49] K. Kumazaki, Phys. Status Solidi B **160**, K173 (1990).
[50] K. Parlinski, J. Łażewski, and Y. Kawazoe, J. Phys. Chem. Solids **61**, 87 (1999).
[51] K. Parlinski, J. Alloys Compd. **328**, 97 (2001).
[52] R. Pick, M.H. Cohen, and R.M. Martin, Phys. Rev. B **1**, 910 (1970).
[53] R. Resta, Ferroelectrics **136**, 51 (1992).
[54] D. Vanderbilt, Phys. Rev. B **41**, 7892 (1990).
[55] G. Kresse and J. Hafner, J. Phys.: Condens. Matter **6**, 8245 (1994).
[56] S.L. Lehoczky, J.G. Broerman, D.A. Nelson, and C.R. Whitsett, Phys. Rev. B **9**, 1598 (1974).
[57] B. Prevot, B. Hennion, and B. Dorner, J. Phys. C **10**, 3999 (1977).
[58] M.M. Elcombe, Proc. R. Soc. London, Ser. A **300**, 210 (1967).
[59] W. Cochran, R.A. Cowley, G. Dolling, and M.M. Elcombe, Proc. R. Soc. London, Ser. A **293**, 433 (1966).
[60] K.S. Upadhyaya, M. Yadav, and G.K. Upadhyaya, Phys. Status Solidi B **229**, 1129 (2002).